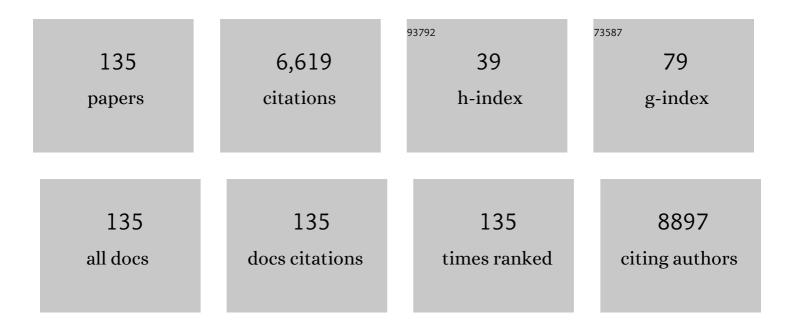
Sanghun Jeon

List of Publications by Year in descending order

Source: https://exaly.com/author-pdf/2593226/publications.pdf Version: 2024-02-01



#	Article	IF	CITATIONS
1	Sub 5 ÃEOT Hf <i>â,"</i> Zr _{1–<i>x</i>} Oâ,, for Next-Generation DRAM Capacitors Using Morphotropic Phase Boundary and High-Pressure (200 atm) Annealing With Rapid Cooling Process. IEEE Transactions on Electron Devices, 2022, 69, 103-108.	1.6	16
2	Verticalâ€Pillar Ferroelectric Fieldâ€Effectâ€Transistor Memory. Physica Status Solidi - Rapid Research Letters, 2022, 16, .	1.2	2
3	Flexible Ferroelectric Hafnia-Based Synaptic Transistor by Focused-Microwave Annealing. ACS Applied Materials & Interfaces, 2022, 14, 1326-1333.	4.0	22
4	Relatively Low- <i>k</i> Ferroelectric Nonvolatile Memory Using Fast Ramping Fast Cooling Annealing Process. IEEE Transactions on Electron Devices, 2022, 69, 3439-3445.	1.6	6
5	Non-Volatile Majority Function Logic Using Ferroelectric Memory for Logic in Memory Technology. IEEE Electron Device Letters, 2022, 43, 1049-1052.	2.2	7
6	High performance ferroelectric field-effect transistors for large memory-window, high-reliability, high-speed 3D vertical NAND flash memory. Journal of Materials Chemistry C, 2022, 10, 9802-9812.	2.7	7
7	Flexible and stretchable conductive fabric for temperature detection. , 2022, , .		2
8	Wearable pressure sensor based on solution-coated fabric for pulse detection. , 2022, , .		3
9	Interfacial Dipole Modulation Device With SiO _X Switching Species. IEEE Journal of the Electron Devices Society, 2021, 9, 57-60.	1.2	0
10	Low-Temperature Growth of Ferroelectric Hf _{0.5} Zr _{0.5} O ₂ Thin Films Assisted by Deep Ultraviolet Light Irradiation. ACS Applied Electronic Materials, 2021, 3, 1244-1251.	2.0	16
11	Effect of Insertion of Dielectric Layer on the Performance of Hafnia Ferroelectric Devices. IEEE Transactions on Electron Devices, 2021, 68, 841-845.	1.6	29
12	Ferroelectricity in Alâ,,Oâ,ƒ/Hf0.5Zr0.5Oâ,, Bilayer Stack: Role of Dielectric Layer Thickness and Annealing Temperature. Journal of Semiconductor Technology and Science, 2021, 21, 62-67.	0.1	9
18	The Influence of Top and Bottom Metal Electrodes on Ferroelectricity of Hafnia. IEEE Transactions on Electron Devices, 2021, 68, 523-528.	1.6	80
14	Insertion of Dielectric Interlayer: A New Approach to Enhance Energy Storage in Hfâ,"Zr _{1-x} Oâ" Capacitors. IEEE Electron Device Letters, 2021, 42, 331-334.	2.2	30
15	Effect of Hydrogen on Hafnium Zirconium Oxide Fabricated by Atomic Layer Deposition Using H ₂ O ₂ Oxidant. Physica Status Solidi - Rapid Research Letters, 2021, 15, 2100020.	1.2	2
16	Highâ€Performance and Highâ€Endurance HfO ₂ â€Based Ferroelectric Fieldâ€Effect Transistor Memory with a Spherical Recess Channel. Physica Status Solidi - Rapid Research Letters, 2021, 15, 2100018.	1.2	15
17	Influence of High-Pressure Annealing Conditions on Ferroelectric and Interfacial Properties of Zr-Rich Hf <i>â, "</i> Zrâ,â,< <i>â, "</i> Oâ,,Capacitors. IEEE Transactions on Electron Devices, 2021, 68, 1996-2002	2. ^{1.6}	27
18	Stress Engineering as a Strategy to Achieve High Ferroelectricity in Thick Hafnia Using Interlayer. IEEE Transactions on Electron Devices. 2021, 68, 2538-2542.	1.6	27

#	Article	IF	CITATIONS
19	Effect of high pressure anneal on switching dynamics of ferroelectric hafnium zirconium oxide capacitors. Journal of Applied Physics, 2021, 129, .	1.1	15
20	Ferroelectricity Enhancement in Hf _{0.5} Zr _{0.5} O ₂ Based Tri-Layer Capacitors at Low-Temperature (350 °C) Annealing Process. IEEE Electron Device Letters, 2021, 42, 812-815.	2.2	39
21	Effect of Ga composition on mobility in a-InGaZnO thin-film transistors. Nanotechnology, 2021, 32, 095201.	1.3	2
22	Selector-less Ferroelectric Tunnel Junctions by Stress Engineering and an Imprinting Effect for High-Density Cross-Point Synapse Arrays. ACS Applied Materials & Interfaces, 2021, 13, 59422-59430.	4.0	28
23	Oxide electronics: Translating materials science from lab-to-fab. MRS Bulletin, 2021, 46, 1028-1036.	1.7	8
24	Enabling large ferroelectricity and excellent reliability for ultra-thin hafnia-based ferroelectrics with a W bottom electrode by inserting a metal-nitride diffusion barrier. Applied Physics Letters, 2021, 119, .	1.5	5
25	High Performance and Self-rectifying Hafnia-based Ferroelectric Tunnel Junction for Neuromorphic Computing and TCAM Applications. , 2021, , .		13
26	Broad spectral responsivity in highly photoconductive InZnO/MoS2 heterojunction phototransistor with ultrathin transparent metal electrode. Nanotechnology, 2020, 31, 035201.	1.3	0
27	Demonstration of High Ferroelectricity (P\$_{{r}\$ ~ 29 \$mu\$ C/cm ²) in Zr Rich Hf _x Zr _{1–x} O ₂ Films. IEEE Electron Device Letters, 2020, 41, 34-37.	2.2	38
28	Improved Ferroelectric Switching in Sputtered HfZrO _x Device Enabled by High Pressure Annealing. IEEE Electron Device Letters, 2020, 41, 232-235.	2.2	18
29	Crystalline Phase-Controlled High-Quality Hafnia Ferroelectric With RuOâ,, Electrode. IEEE Transactions on Electron Devices, 2020, 67, 3431-3434.	1.6	29
30	Trade-off between interfacial charge and negative capacitance effects in the Hf-Zr-Al-O/Hf0.5Zr0.5O2 bilayer system. Solid-State Electronics, 2020, 174, 107914.	0.8	14
31	Metal-induced n+/n homojunction for ultrahigh electron mobility transistors. NPG Asia Materials, 2020, 12, .	3.8	6
32	Excellent Reliability and High-Speed Antiferroelectric HfZrO ₂ Tunnel Junction by a High-Pressure Annealing Process and Built-In Bias Engineering. ACS Applied Materials & Interfaces, 2020, 12, 57539-57546.	4.0	37
33	High-k Hf _x Zr _{1-x} Oâ,, Ferroelectric Insulator by Utilizing High Pressure Anneal. IEEE Transactions on Electron Devices, 2020, 67, 2489-2494.	1.6	36
34	Ferroelectricity Enhancement in Hf _{0.5} Zr _{0.5} O ₂ Capacitors by Incorporating Ta ₂ O ₅ Dielectric Seed Layers. , 2020, , .		8
35	Effect of Forming Gas High-Pressure Annealing on Metal-Ferroelectric-Semiconductor Hafnia Ferroelectric Tunnel Junction. IEEE Electron Device Letters, 2020, 41, 1193-1196.	2.2	43
36	Oxygen vacancy control as a strategy to achieve highly reliable hafnia ferroelectrics using oxide electrode. Nanoscale, 2020, 12, 9024-9031.	2.8	98

#	Article	IF	CITATIONS
37	Flexible multimodal sensor inspired by human skin based on hair-type flow, temperature, and pressure. Flexible and Printed Electronics, 2020, 5, 025003.	1.5	21
38	Effect of High Pressure Annealing Temperature on the Ferroelectric Properties of TiN/Hf _{0.25} Zr _{0.75} O ₂ /TiN Capacitors. , 2020, , .		2
39	Metallic Glass-Based Dual-Mode Sensor for Soft Electronics. IEEE Sensors Journal, 2020, 20, 12396-12401.	2.4	2
40	Evolution of crystallographic structure and ferroelectricity of Hf0.5Zr0.5O2 films with different deposition rate. AIP Advances, 2020, 10, .	0.6	22
41	Insertion of HfO ₂ Seed/Dielectric Layer to the Ferroelectric HZO Films for Heightened Remanent Polarization in MFM Capacitors. IEEE Transactions on Electron Devices, 2020, 67, 745-750.	1.6	67
42	Silk-Based Self Powered Pressure Sensor for Applications in Wearable Device. , 2020, , .		2
43	Ultra-thin Hf0.5Zr0.5O2 thin-film-based ferroelectric tunnel junction via stress induced crystallization. Applied Physics Letters, 2020, 117, .	1.5	83
44	(Invited) Hafnia Ferroelectric Device for Semiconductor, Sensor, and Display Applications. ECS Transactions, 2020, 98, 219-223.	0.3	4
45	Influence of High-Pressure Annealing on Memory Properties of Hf _{0.5} Zr _{0.5} O ₂ Based 1T-FeRAM. IEEE Electron Device Letters, 2019, 40, 1076-1079.	2.2	10
46	Transparent and Flexible Mayan-Pyramid-based Pressure Sensor using Facile-Transferred Indium tin Oxide for Bimodal Sensor Applications. Scientific Reports, 2019, 9, 14040.	1.6	24
47	Comprehensive study of high pressure annealing on the ferroelectric properties of Hf _{0.5} Zr _{0.5} O ₂ thin films. Nanotechnology, 2019, 30, 505204.	1.3	9
48	Opportunity of Metallic Glass in Soft Electronics. , 2019, , .		0
49	Flexible Multi-Modal Sensor for Electronic Skin. , 2019, , .		1
50	Flexible Multimodal Sensors for Electronic Skin: Principle, Materials, Device, Array Architecture, and Data Acquisition Method. Proceedings of the IEEE, 2019, 107, 2065-2083.	16.4	59
51	Improved optical performance of multi-layer MoS2 phototransistor with see-through metal electrode. Nano Convergence, 2019, 6, 32.	6.3	9
52	Amorphous FeZr metal for multi-functional sensor in electronic skin. Npj Flexible Electronics, 2019, 3,	5.1	18
53	Robust and scalable three-dimensional spacer textile pressure sensor for human motion detection. Smart Materials and Structures, 2019, 28, 065019.	1.8	37
54	Effects of high pressure nitrogen annealing on ferroelectric Hf0.5Zr0.5O2 films. Applied Physics Letters, 2018, 112, .	1.5	52

#	Article	IF	CITATIONS
55	Resistive switching characteristics of a modified active electrode and Ti buffer layer in Cu Se-based atomic switch. Journal of Alloys and Compounds, 2018, 753, 551-557.	2.8	13
56	Enhancement of resistive switching properties in Al ₂ O ₃ bilayer-based atomic switches: multilevel resistive switching. Nanotechnology, 2018, 29, 235202.	1.3	46
57	Excellent Resistive Switching Performance of Cu–Se-Based Atomic Switch Using Lanthanide Metal Nanolayer at the Cu–Se/Al ₂ O ₃ Interface. ACS Applied Materials & Interfaces, 2018, 10, 8124-8131.	4.0	14
58	Pulse Switching Study on the HfZrO Ferroelectric Films With High Pressure Annealing. IEEE Transactions on Electron Devices, 2018, 65, 1771-1773.	1.6	52
59	Quantitative analysis of charge trapping and classification of sub-gap states in MoS ₂ TFT by pulse <i>I</i> – <i>V</i> method. Nanotechnology, 2018, 29, 175704.	1.3	14
60	Scalable and facile synthesis of stretchable thermoelectric fabric for wearable self-powered temperature sensors. RSC Advances, 2018, 8, 39992-39999.	1.7	58
61	Discharge Current Analysis Estimating the Defect Sites in Amorphous Hafnia Thin-Film Transistor. IEEE Transactions on Electron Devices, 2018, 65, 3264-3268.	1.6	0
62	First-order reversal curve diagrams for characterizing ferroelectricity of Hf0.5Zr0.5O2 films grown at different rates. Journal of Vacuum Science and Technology B:Nanotechnology and Microelectronics, 2018, 36, .	0.6	12
63	The effect of the bottom electrode on ferroelectric tunnel junctions based on CMOS-compatible HfO ₂ . Nanotechnology, 2018, 29, 335201.	1.3	120
64	Enhanced tunneling electroresistance effects in HfZrO-based ferroelectric tunnel junctions by high-pressure nitrogen annealing. Applied Physics Letters, 2018, 113, .	1.5	51
65	Effect of dysprosium and lutetium metal buffer layers on the resistive switching characteristics of Cu–Sn alloy-based conductive-bridge random access memory. Nanotechnology, 2018, 29, 385207.	1.3	5
66	Non-volatile resistive switching in CuBi-based conductive bridge random access memory device. Applied Physics Letters, 2018, 112, 253503.	1.5	6
67	Defects and Charge-Trapping Mechanisms of Double-Active-Layer In–Zn–O and Al–Sn–Zn–In–O Thin-Film Transistors. ACS Applied Materials & Interfaces, 2017, 9, 9271-9279.	4.0	20
68	Polymer-Assisted Solution Processing of TiO ₂ Thin Films for Resistive-Switching Random Access Memory. Journal of the Electrochemical Society, 2017, 164, H21-H24.	1.3	9
69	HfZrO _{<italic>x</italic>} -Based Ferroelectric Synapse Device With 32 Levels of Conductance States for Neuromorphic Applications. IEEE Electron Device Letters, 2017, 38, 732-735.	2.2	202
70	Determination of intrinsic mobility of a bilayer oxide thin-film transistor by pulsed I–V method. Nanotechnology, 2017, 28, 175201.	1.3	4
71	Influence of Fast Charging on Accuracy of Mobility in \${a}\$ -InHfZnO Thin-Film Transistor. IEEE Electron Device Letters, 2017, 38, 203-206.	2.2	16
72	Microsecond Pulse I–V Approach to Understanding Defects in High Mobility Bi-layer Oxide Semiconductor Transistor. Scientific Reports, 2017, 7, 8235.	1.6	7

#	Article	IF	CITATIONS
73	Impact of fast transient charging and ambient on mobility of WS2 field-effect transistor. Journal of Vacuum Science and Technology B:Nanotechnology and Microelectronics, 2017, 35, .	0.6	8
74	Low-voltage, high-sensitivity and high-reliability bimodal sensor array with fully inkjet-printed flexible conducting electrode for low power consumption electronic skin. Nano Energy, 2017, 41, 301-307.	8.2	104
75	Fast and slow transient charging of Oxide Semiconductor Transistors. Scientific Reports, 2017, 7, 11850.	1.6	10
76	Paper-Based Bimodal Sensor for Electronic Skin Applications. ACS Applied Materials & Interfaces, 2017, 9, 26974-26982.	4.0	83
77	Sub-60-mV/decade Negative Capacitance FinFET With Sub-10-nm Hafnium-Based Ferroelectric Capacitor. IEEE Journal of the Electron Devices Society, 2017, 5, 306-309.	1.2	57
78	Poly-4-vinylphenol (PVP) and Poly(melamine- <i>co</i> -formaldehyde) (PMF)-Based Atomic Switching Device and Its Application to Logic Gate Circuits with Low Operating Voltage. ACS Applied Materials & Interfaces, 2017, 9, 27073-27082.	4.0	25
79	Vertically stacked nanocellulose tactile sensor. Nanoscale, 2017, 9, 17212-17219.	2.8	55
80	Efficient Suppression of Defects and Charge Trapping in High Density In–Sn–Zn–O Thin Film Transistor Prepared using Microwave-Assisted Sputter. ACS Applied Materials & Interfaces, 2017, 9, 36962-36970.	4.0	8
81	Effect of hydrogen on dynamic charge transport in amorphous oxide thin film transistors. Nanotechnology, 2016, 27, 325203.	1.3	13
82	Photosensitivity of InZnO thin-film transistors using a solution process. Applied Physics Letters, 2016, 109, .	1.5	30
83	The influence of interfacial defects on fast charge trapping in nanocrystalline oxide-semiconductor thin film transistors. Semiconductor Science and Technology, 2016, 31, 055014.	1.0	15
84	Beneficial effect of hydrogen in aluminum oxide deposited through the atomic layer deposition method on the electrical properties of an indium–gallium–zinc oxide thin-film transistor. Journal of Information Display, 2016, 17, 65-71.	2.1	36
85	The Influence of Hydrogen on Defects of In–Ga–Zn–O Semiconductor Thin-Film Transistors With Atomic-Layer Deposition of Al ₂ O ₃ . IEEE Electron Device Letters, 2016, 37, 1131-1134.	2.2	28
86	Light illumination effect in AIZTO/IZO dual-channel TFTs. , 2016, , .		0
87	III–V compound semiconductors for mass-produced nano-electronics: theoretical studies on mobility degradation by dislocation. Scientific Reports, 2016, 6, 22001.	1.6	17
88	High mobility and high stability glassy metal-oxynitride materials and devices. Scientific Reports, 2016, 6, 23940.	1.6	24
89	Dislocation effects in FinFETs for different III–V compound semiconductors. Journal Physics D: Applied Physics, 2016, 49, 155101.	1.3	2
90	Pulse <i>I</i> – <i>V</i> characterization of a nano-crystalline oxide device with sub-gap density of states. Nanotechnology, 2016, 27, 215203.	1.3	9

#	Article	IF	CITATIONS
91	Oxygen Defect-Induced Metastability in Oxide Semiconductors Probed by Gate Pulse Spectroscopy. Scientific Reports, 2015, 5, 14902.	1.6	53
92	A Sensor Array Using Multi-functional Field-effect Transistors with Ultrahigh Sensitivity and Precision for Bio-monitoring. Scientific Reports, 2015, 5, 12705.	1.6	79
93	Fast transient charging behavior of HfInZnO thin-film transistor. Applied Physics Letters, 2015, 107, .	1.5	23
94	Ar plasma treated ZnON transistor for future thin film electronics. Applied Physics Letters, 2015, 107, .	1.5	52
95	A Monte Carlo simulation for bipolar resistive memory switching in large band-gap oxides. Applied Physics Letters, 2015, 107, .	1.5	3
96	A combinatorial device analysis method of oxide thin-film transistors. , 2015, , .		0
97	45.3: <i>Invited Paper</i> : High Performance Nanocrystalline ZnO _x N _y for Imaging and Display Applications. Digest of Technical Papers SID International Symposium, 2015, 46, 681-684.	0.1	0
98	Oxide thin film transistor technology: Capturing device-circuit interactions. , 2015, , .		0
99	Transparent Semiconducting Oxide Technology for Touch Free Interactive Flexible Displays. Proceedings of the IEEE, 2015, 103, 644-664.	16.4	85
100	Anomalous high photoconductivity in short channel indium-zinc-oxide photo-transistors. Applied Physics Letters, 2015, 106, .	1.5	16
101	Photoresponse of an oxide semiconductor photosensor. Journal of Vacuum Science and Technology B:Nanotechnology and Microelectronics, 2015, 33, .	0.6	14
102	Field-induced macroscopic barrier model for persistent photoconductivity in nanocrystalline oxide thin-film transistors. Applied Physics Letters, 2014, 104, .	1.5	20
103	Fourier spectrum based extraction of an equivalent trap state density in indium gallium zinc oxide transistors. Applied Physics Letters, 2014, 104, 203505.	1.5	1
104	Origin of High Photoconductive Gain in Fully Transparent Heterojunction Nanocrystalline Oxide Image Sensors and Interconnects. Advanced Materials, 2014, 26, 7102-7109.	11.1	65
105	Thickness dependent low-frequency noise characteristics of <i>a</i> -InZnO thin-film transistors under light illumination. Applied Physics Letters, 2014, 104, 023505.	1.5	12
106	Amorphous Oxide Semiconductor TFTs for Displays and Imaging. Journal of Display Technology, 2014, 10, 917-927.	1.3	133
107	Highly Stretchable Resistive Pressure Sensors Using a Conductive Elastomeric Composite on a Micropyramid Array. Advanced Materials, 2014, 26, 3451-3458.	11.1	1,030
108	Nanocrystalline ZnON; High mobility and low band gap semiconductor material for high performance switch transistor and image sensor application. Scientific Reports, 2014, 4, 4948.	1.6	82

#	Article	IF	CITATIONS
109	A Flexible Bimodal Sensor Array for Simultaneous Sensing of Pressure and Temperature. Advanced Materials, 2014, 26, 796-804.	11.1	375
110	Nano-Crystalline Oxide Semiconductor Materials for Display and Semiconductor Device Applications. ECS Meeting Abstracts, 2014, , .	0.0	0
111	Modeling Sub-Threshold Current–Voltage Characteristics in Thin Film Transistors. Journal of Display Technology, 2013, 9, 883-889.	1.3	42
112	Highâ€Performance Nanowire Oxide Photoâ€Thin Film Transistor. Advanced Materials, 2013, 25, 5549-5554.	11.1	49
113	Impact of transparent electrode on photoresponse of ZnO-based phototransistor. Applied Physics Letters, 2013, 103, 251111.	1.5	17
114	Oxide electronics for imaging and displays. , 2013, , .		0
115	The impact of active layer thickness on low-frequency noise characteristics in InZnO thin-film transistors with high mobility. Applied Physics Letters, 2012, 100, .	1.5	38
116	Gated three-terminal device architecture to eliminate persistent photoconductivity in oxide semiconductor photosensor arrays. Nature Materials, 2012, 11, 301-305.	13.3	434
117	Highly stretchable electric circuits from a composite material of silver nanoparticles and elastomeric fibres. Nature Nanotechnology, 2012, 7, 803-809.	15.6	782
118	Metal Oxide Thin Film Phototransistor for Remote Touch Interactive Displays. Advanced Materials, 2012, 24, 2631-2636.	11.1	143
119	Verification of Interface State Properties of a-InGaZnO Thin-Film Transistors With \$hbox{SiN}_{x}\$ and \$ hbox{SiO}_{2}\$ Gate Dielectrics by Low-Frequency Noise Measurements. IEEE Electron Device Letters, 2011, 32, 1083-1085.	2.2	48
120	Nanometer-Scale Oxide Thin Film Transistor with Potential for High-Density Image Sensor Applications. ACS Applied Materials & Interfaces, 2011, 3, 1-6.	4.0	70
121	Highly Manufacturable Device Isolation Technology Using Laser-Induced Epitaxial Growth for Monolithic Stack Devices. IEEE Transactions on Electron Devices, 2011, 58, 3863-3868.	1.6	1
122	Short channel device performance of amorphous InGaZnO thin film transistor. Applied Physics Letters, 2011, 99, .	1.5	41
123	Influence of Hf contents on interface state properties in <i>a</i> -HfInZnO thin-film transistors with SiNx/SiOx gate dielectrics. Applied Physics Letters, 2011, 99, .	1.5	32
124	Fully transparent InGaZnO thin film transistors using indium tin oxide/graphene multilayer as source/drain electrodes. Applied Physics Letters, 2010, 97, .	1.5	21
125	Instability in threshold voltage and subthreshold behavior in Hf–In–Zn–O thin film transistors induced by bias-and light-stress. Applied Physics Letters, 2010, 97, .	1.5	108
126	Low-Frequency Noise Performance of a Bilayer InZnO–InGaZnO Thin-Film Transistor for Analog Device Applications. IEEE Electron Device Letters, 2010, 31, 1128-1130.	2.2	58

#	Article	IF	CITATIONS
127	High performance low voltage amorphous oxide TFT Enhancement/Depletion inverter through uni-/bi-layer channel hybrid integration. , 2009, , .		12

128 Effect of hygroscopic nature on the electrical characteristics of lanthanide oxides (Pr2O3, Sm2O3,) Tj ETQq0 0 0 rgBT /Overlock 10 Tf 50

129	Electrical characteristics of ZrO2 prepared by electrochemical anodization of Zr in an ammonium tartrate electrolyte. Journal of Vacuum Science and Technology A: Vacuum, Surfaces and Films, 2003, 21, L5-L9.	0.9	9
130	Electrical characteristics of ultrathin ZrO[sub 2] prepared by wet oxidation of an ultrathin Zr-metal layer. Journal of Vacuum Science & Technology an Official Journal of the American Vacuum Society B, Microelectronics Processing and Phenomena, 2002, 20, 400.	1.6	11
131	Electrical and physical characteristics of PrTixOy for metal-oxide-semiconductor gate dielectric applications. Applied Physics Letters, 2002, 81, 4856-4858.	1.5	59
132	Electrical characteristics of ZrOxNy prepared by NH3 annealing of ZrO2. Applied Physics Letters, 2001, 79, 245-247.	1.5	91
133	Electrical characteristics of a Dy-doped HfO2 gate dielectric. Applied Physics Letters, 2001, 79, 2615-2617.	1.5	22
134	Electrical Characteristics of TaOxNy for High-k MOS Gate Dielectric Applications. Materials Research Society Symposia Proceedings, 2000, 611, 1.	0.1	0
135	Excellent electrical characteristics of lanthanide (Pr, Nd, Sm, Gd, and Dy) oxide and lanthanide-doped oxide for MOS gate dielectric applications. , 0, , .		6